JOURNAL OF MAGNETIC RESONANCE **124,** 200–204 (1997)
ARTICLE NO. MN967495

NOTES

Investigation of Uncertainties in Relaxation Analysis of 2D NOE Which Arise from Spectral Noise

VLADIMIR A. LIKIĆ AND FRANKLYN G. PRENDERGAST

Guggenheim 14, Department of Biochemistry and Molecular Biology, Mayo Graduate School, Mayo Foundation, Rochester, Minnesota 55905

Received March 18, 1996; revised September 30, 1996

Two-dimensional NOE spectroscopy is a valuable technique for investigation of biological macromolecules in solution (*1, 2*). A 2D NOE spectrum can be viewed as a matrix of peak volumes (*3, 4*)

$$\mathbf{a}(\tau_m) = \exp[-\mathbf{R}\tau_m]\mathbf{a}(0), \qquad [1]$$

where τ_m represents the mixing time, $\mathbf{R}$ is the relaxation matrix, and $\mathbf{a}(0)$ is the matrix of peak volumes for $\tau_m = 0$. Off-diagonal elements of the relaxation matrix are cross-relaxation (CR) rates which allow estimation of internuclear distances, the latter being essential inputs for macromolecular structure determination by NMR. There are two standard methods for the estimation of CR rates from the experimentally measured mixing matrix $\mathbf{a}(\tau_m)$: initial slope approximation (*3, 5, 6*) and relaxation-matrix analysis (*4, 7–12*). Initial-slope approximation is based on the truncated series expansion of the matrix exponential from Eq. [1] and is valid only for short mixing times (*3, 5, 10*). Relaxation-matrix analysis inverts Eq. [1] and gives an exact solution for the relaxation matrix (*4, 10*)

$$\mathbf{R} = -\frac{1}{\tau_m}\ln[\mathbf{a}(\tau_m)\mathbf{a}^{-1}(0)]. \qquad [2]$$

High quality of spatial constraints is essential for high resolution of macromolecular structures obtained from NMR data (*13–15*). Cross-relaxation rates contain information about molecular dynamics (*16–18*) and are interesting for their own sake. It is therefore highly desirable to measure CR rates both accurately and precisely. Accordingly, the propagation of errors in the relaxation analysis of 2D NOE (*13, 19*), and its influence on derived interproton distances (*20–22*), is an important problem. In this particular context, propagation of errors refers to the propagation of uncertainties in experimentally measured peak volumes into the CR rates obtained by relaxation analysis.

Uncertainties in estimated CR rates are generated by (i) errors in measurement of peak volumes, and (ii) errors introduced by the approximations used in the relaxation analysis. The errors in measured peak volumes arise due to presence of spectral noise (*13, 19*), overlap of peak volumes (*13*), finite spectral resolution (*13*), and possible systematic errors (*23*). At present, overlap of spectral peaks severely limits the application of relaxation-matrix analysis which requires a complete mixing matrix as input. The initial-slope method is less sensitive to this problem, since it can be independently applied to well-resolved spectral peaks. In this Communication, we investigate errors which arise solely from spectral noise, and we ignore other possible sources of errors in the measurement of peak volumes. This choice is motivated by the ubiquitous presence of spectral noise (which equally affects the initial-slope and relaxation-matrix methods, and therefore allows their straightforward comparison), and by the recently derived equation for propagation of errors in the relaxation-matrix analysis (*19*).

Spectral noise introduces an uncertainty in measured peak volumes, which, in turn, generates an uncertainty in calculated CR rates. We focus on the transmittal of those errors by the logarithm in Eq. [2], especially in the context of protein structure determination. We show that (i) an increase in protein size inevitably leads to an increase in the uncertainty of estimated CR rates, and (ii) for remote methylene protons, which account for up to one-third of all the CR rates useful for structure determination, the initial-slope approximation may give a better result than relaxation-matrix analysis. This latter point is unexpected because the initial-slope approximation is itself essentially an approximation of the relaxation-matrix analysis. However, the errors in two methods propagate differently, and initial-slope approximation may be compensated from the approximations used by a more favorable propagation of errors.

An equation for the propagation of small random errors in

1090-7807/97 $25.00

Eq. [2] has been described in Ref. (*19*). This equation gives the uncertainty in calculated CR rates as a function of the eigenvalues λ_i and eigenvectors u_i of the relaxation matrix

$$\Delta R_{ij} = \Delta a \left\{ \sum_{k=1}^{N} \sum_{l=1}^{N} u_{ik}^2 u_{jl}^2 \times \left[\frac{\lambda_k - \lambda_l}{\exp(-\lambda_k \tau_m) - \exp(-\lambda_l \tau_m)} \right]^2 \right\}^{1/2}. \quad [3]$$

ΔR_{ij} refers to the element R_{ij} of the relaxation matrix **R**, Δa is the error in measurement of peak volumes, and u_{ik} denotes the kth element of the normalized eigenvector that belongs to the eigenvalue λ_i. Since **R** is symmetric, Eq. [3] implies that $\Delta R_{ij} = \Delta R_{ji}$ for $i, j = 1, 2, \ldots, N$.

Consider the hypothetical four-spin system, depicted in Fig. 1a, where σ and σ_1 denote cross-relaxation rates. We shall assume the slow motional limit ($\omega\tau_c \gg 1$, valid for macromolecules in high magnetic fields), and that external relaxation is negligible. From Fig. 1, it follows that $R_{12} = \sigma_1$, $R_{13} = R_{14} = R_{23} = R_{24} = R_{34} = \sigma$, $R_{11} = R_{22} = -(\sigma_1 + 2\sigma)$, and $R_{33} = R_{44} = -3\sigma$. This cumbersome notation is needed because, for example, although R_{13} and R_{34} are equal, errors associated with them are not. From the relaxation matrix (whose elements are R_{ij}), one can find its eigenvalues λ_i and eigenvectors u_i, and application of Eq. [3] yields

$$\Delta R_{12} = \Delta a \left\{ \frac{2\sigma^2}{[\exp(4\sigma\tau_m) - 1]^2} + \frac{(\sigma - \sigma_1)^2}{\exp[4(3\sigma + \sigma_1)\tau_m] \times [\exp(-2(\sigma + \sigma_1)\tau_m) - \exp(-4\sigma\tau_m)]^2} + \frac{(\sigma_1 + \sigma)^2}{[\exp(2(\sigma_1 + \sigma)\tau_m) - 1]^2} + \frac{1 + \exp(-8\sigma\tau_m) + 4\exp[-4(\sigma + \sigma_1)\tau_m]}{16\tau_m^2} \right\}^{1/2}, \quad [4a]$$

$$\Delta R_{13} = \Delta R_{14} = \Delta R_{23} = \Delta R_{24} = \Delta a \left\{ \frac{4\sigma^2}{[\exp(4\sigma\tau_m) - 1]^2} + \frac{1 + 3\exp(-8\sigma\tau_m)}{16\tau_m^2} + \frac{3(\sigma_1 - \sigma)^2}{2[\exp(2(\sigma + \sigma_1)\tau_m) - \exp(4\sigma\tau_m)]^2} + \frac{(\sigma_1 + \sigma)^2}{2[\exp(2(\sigma_1 + \sigma)\tau_m) - 1]^2} \right\}^{1/2}, \quad [4b]$$

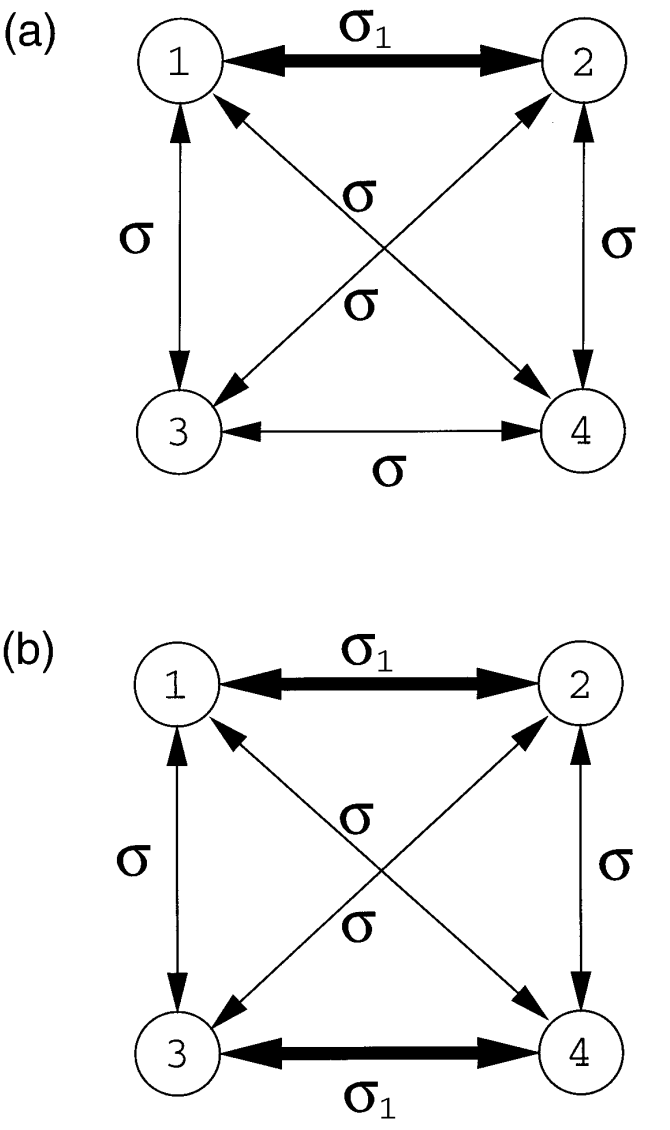

FIG. 1. Two model spin systems discussed in the text. The case of interest is when $|\sigma_1| \gg |\sigma|$. The connection between σ_1, σ and the elements of the relaxation matrix **R** is the following: (a) $R_{12} = \sigma_1$, $R_{13} = R_{14} = R_{23} = R_{24} = R_{34} = \sigma$; (b) $R_{12} = R_{34} = \sigma_1$ and $R_{13} = R_{14} = R_{23} = R_{24} = \sigma$.

$$\Delta R_{34} = \Delta a \left\{ \frac{6\sigma^2}{[\exp(4\sigma\tau_m) - 1]^2} + \frac{1 + 9\exp(-8\sigma\tau_m)}{16\tau_m^2} \right\}^{1/2}. \quad [4c]$$

The uncertainty ΔR_{12} increases as $|R_{12}| = |\sigma_1|$ increases, and the relative error $\Delta R_{12}/R_{12}$ (for some optimal and fixed mixing time) does not change much. However, Eqs. [4b] and [4c] show that ΔR_{13}, ΔR_{14}, ΔR_{23}, and ΔR_{24} also depend

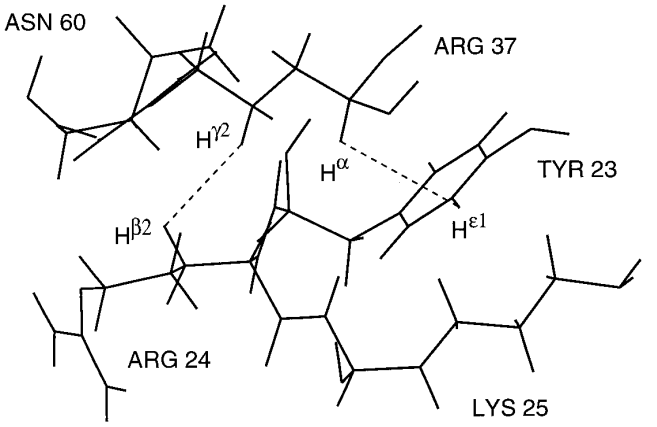

FIG. 2. Residues participating in the 4.5 Å sphere used in computer simulations. Relative positions of examined spin pairs ARG^{37} $H^{\gamma 2}$–ARG^{24} $H^{\beta 2}$ and ARG^{37} H^{α}–TYR^{23} $H^{\epsilon 1}$ are shown.

upon σ_1 while ΔR_{34} does not. Specifically, as $|\sigma_1| = |R_{12}|$ increases, uncertainties ΔR_{13}, ΔR_{14}, ΔR_{23}, and ΔR_{24} also increase. In the limit $|\sigma_1| \gg |\sigma|$, both absolute and relative errors for R_{13}, R_{14}, R_{23}, and R_{24} become much larger than those for R_{34}. This is a consequence of the effect of a spectator spin described previously in the three-spin system (*22*). Note that this error arises because R_{13}, R_{14}, R_{23}, and R_{24} share one spin with the strong cross-relaxation R_{12}. The error ΔR_{34} is unaffected by $R_{12} = \sigma_1$, as Eq. [4c] shows. In proteins, this effect would influence the CR rate which connects a methylene proton and some close nonmethylene proton (see below).

The related question concerns the CR rates which share both of its spins with the two much stronger CR rates. Such a case occurs for CR rates connecting two *remote* methylene protons, and the hypothetical four-spin system shown in Fig. 1b may serve as a model. Application of Eq. [3] yields Eq. [4a] for the uncertainties in all six cross-relaxation rates; absolute errors ΔR_{13}, ΔR_{14}, ΔR_{23}, and ΔR_{24} are equal to ΔR_{12} (ΔR_{34}). Therefore, if $|\sigma_1| \gg |\sigma|$, relative errors $\Delta R_{13}/\sigma$, $\Delta R_{14}/\sigma$, $\Delta R_{23}/\sigma$, and $\Delta R_{24}/\sigma$ become very large.

We want to stress that this increase in relative errors is solely due to the influence of strong CR rates R_{12} and R_{34}, with whom R_{13}, R_{14}, R_{23}, and R_{24} share a spin. In the first example (Fig. 1a and Eq. [4c]), the uncertainty ΔR_{34} remains unaffected, since R_{34} shares no spin with the strong CR rate R_{12}. By the same token, in the second example, R_{13}, R_{14}, R_{23}, and R_{24} are under the double influence of strong CR rates R_{12} and R_{34}. We refer to this as the effect of remote methylene protons. Because of the $1/r^6$ dependence of CR rates, methylene ($>CH_2$) proton pairs exhibit much stronger cross relaxation than other proton pairs in a protein; therefore, the effect of remote methylene protons will impact CR rates between protons that belong to different methylene groups.

In the limit $\sigma_1 \to \sigma$, Eqs. [4a] and [4b] collapse into Eq. [4c], which gives the uncertainty in the four-spin system when all CR rates equal σ. As a logical extension, one can consider several spin systems which differ in the number of spins, when all CR rates are the same and equal to σ. In three-dimensional space, this is impossible for $N > 4$. However, the effects discussed here are inherent in the matrix logarithm from Eq. [2] and do not depend upon the possible spin arrangements; hence, such limits can be used to obtain qualitative behavior. Thus, the solution of Eq. [3] gives the error in σ as a function of the size of the spin system (N):

$$\Delta R_{ij} = \Delta a \left\{ \frac{2(N-1)\sigma^2}{[\exp(N\sigma\tau_m) - 1]^2} + \frac{1 + (N-1)^2 \exp(-2N\sigma\tau_m)}{N^2\tau_m^2} \right\}^{1/2}, \qquad [5]$$

where $i, j = 1, 2, \ldots, N$ (note that in the slow-motion limit $\sigma < 0$, and Eq. [5] is an exponentially rising function). Equation [5] shows that the uncertainty in the calculated relaxation matrix steadily increases with the size of the spin system. Consequently, for a given level of spectral noise, there is a theoretical limit in the size of the spin system which can be successfully treated by relaxation-matrix analysis.

An increase in the size of the spin system will result in many interproton distances greater than 5 Å, which do not

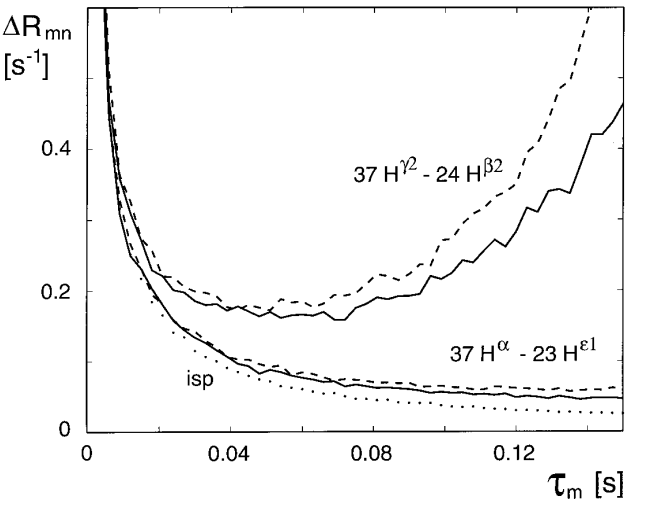

FIG. 3. Computer simulations of the model protein fasciculin 1. Shown are the standard deviations versus mixing time for the 4.5 Å sphere model (full line), 8.0 Å sphere model (broken line), and the isolated spin pair with the interproton distance of 3.14 Å (dots, labeled isp). Due to the influence of methylene partners ARG^{37} $H^{\gamma 1}$ and ARG^{24} $H^{\beta 1}$, ARG^{37} $H^{\gamma 2}$–ARG^{24} $H^{\beta 2}$ cross-relaxation rate is determined with uncertainty several fold larger than that of ARG^{37} H^{α}–TYR^{23} $H^{\epsilon 1}$. See text for more details about the computer simulations.

TABLE 1

Selected Results Obtained from the Computer Simulations of the Relaxation-Matrix Analysis and Quadratic Two-Spin Approximation for a 4.5 Å Sphere in the Presence of 0.5% Spectral Noise

Protons	R_{ij} (s^{-1})[a]	ΔR_{ij} (s^{-1})[b]	Distance (Å)[c]
	X-ray structure		
37 H^{α}–23$H^{\epsilon 1}$	−0.292	N/A	3.145
37$H^{\gamma 2}$–24$H^{\beta 2}$	−0.296	N/A	3.138
	Relaxation-matrix analysis,[d] τ_m = 60 ms		
37H^{α}–23$H^{\epsilon 1}$	−0.294	0.078	3.02–3.31
37$H^{\gamma 2}$–24$H^{\beta 2}$	−0.294	0.168	2.91–3.62
	Relaxation-matrix analysis,[d] τ_m = 150 ms		
37H^{α}–23$H^{\epsilon 1}$	−0.293	0.048	3.07–3.24
37$H^{\gamma 2}$–24$H^{\beta 2}$	−0.262	0.466	>2.70
	Quadratic two-spin approximation,[e] τ_m = 40, 80, 120 ms		
37H^{α}–23$H^{\epsilon 1}$	−0.279	0.100	3.01–3.41
37$H^{\gamma 2}$–24$H^{\beta 2}$	−0.250	0.101	3.05–3.52

[a] The mean for computer simulations.

[b] The standard deviation for computer simulations.

[c] Distance ranges were calculated as to correspond to mean ± standard deviation.

[d] The standard deviation for ARG^{37} $H^{\gamma 2}$–ARG^{24} $H\beta^2$ has a minimum at τ_m = 60 ms (see Fig. 2). For each mixing time, the relaxation-matrix analysis was repeated 500 times.

[e] Three 2D NOE spectra were assumed (τ_m = 40, 80, and 120 ms), and the analysis was repeated 10^4 times.

give rise to NOE cross peaks; i.e., many off-diagonal elements of the relaxation matrix (CR rates) will be zero for practical purposes. If there is some prior information about the molecular spatial structure, the spectral peaks which correspond to protons further than 5 Å apart can be preset to zero, and therefore would not contribute to the propagation of errors. Our conclusion regarding Eq. [5], however, rests on the assumption that no prior information about the molecular spatial structure is available; the volumes of spectral peaks which enter the relaxation-matrix analysis are never zero, but possibly are below the level of spectral noise. Therefore, for an N-spin system, the volumes of all N^2 spectral peaks contribute to the error in CR rates.

We studied the influence of these effects by using the small protein fasciculin 1 (*24*) as a model. We simulated the volumes of cross and diagonal peaks to which the prescribed spectral noise was added. Since simulations with the complete relaxation matrix were not feasible, a limited set of proton resonances was selected with a sphere from the protein interior (*13*). We used two spheres with a common center and radii of 4.5 and 8.0 Å, which include 15 and 68 NMR proton resonances, respectively. Methyl groups were treated as geometrically averaged pseudoatoms. Rigid body isotropic tumbling with a correlation time of 5.0 ns, a spectrometer frequency of 500 MHz, and an external relaxation of 0.2 s^{-1} was assumed. The noise was taken to follow a Gaussian distribution, with a standard deviation of 0.005 (0.5%) relative to the volume of diagonal peaks at τ_m = 0. For each mixing time, an average of 500 relaxation-matrix evaluations was calculated.

Both spheres include ARG^{37} H^{α}, ARG^{37} $H^{\gamma 1}$, ARG^{37} $H^{\gamma 2}$, ARG^{24} $H^{\beta 1}$, ARG^{24} $H^{\beta 2}$, and TYR^{23} $H^{\epsilon 1}$. The distances between protons ARG^{37} $H^{\gamma 2}$–ARG^{24} $H^{\beta 2}$ and ARG^{37} H^{α}–TYR^{23} $H^{\epsilon 1}$ are 3.15 and 3.14 Å, which can be considered equal for practical purposes. Hence, the difference in uncertainties in their determination arises solely from the effect of remote methylene protons, which affects only the CR rate of ARG^{37} $H^{\gamma 2}$–ARG^{24} $H^{\beta 2}$. Figure 2 shows five residues participating in the 4.5 Å sphere, and relative positions of examined spin pairs ARG^{37} $H^{\gamma 2}$–ARG^{24} $H^{\beta 2}$ and ARG^{37} H^{α}–TYR^{23} $H^{\epsilon 1}$.

Figure 3 shows that the uncertainty in the determination of the CR rate ARG^{37} $H^{\gamma 2}$–ARG^{24} $H^{\beta 2}$ is 2–10 times larger than that for ARG^{37} H^{α}–TYR^{23} $H^{\epsilon 1}$, depending on the mixing time. (Since the two CR rates are nearly equal, this holds for both absolute and relative errors.) The increase in the uncertainties for the 8.0 Å relative to the 4.5 Å sphere is solely due to the augmented size of the spin system. The uncertainty for ARG^{37} H^{α}–TYR^{23} $H^{\epsilon 1}$ CR rate is slightly larger than the uncertainty observed for the isolated spin pair featuring the same distance (Fig. 3). Table 1 shows the uncertainties in calculated CR rates and corresponding distance intervals for the 4.5 Å sphere.

At short mixing times, the matrix logarithm can be ap-

proximated with the first few terms of the series expansion, and the initial-slope approximation is valid. In that regime, all interactions are pairwise and the influence of the effect of remote methylene protons is negligible. The linear two-spin approximation, in which only the first term of the series expansion of the matrix exponential is retained, is inferior to the relaxation-matrix treatment (*10, 11, 13, 14, 25*). We examined a quadratic two-spin approximation (*6*), under conditions similar to those of the relaxation-matrix analysis. We assumed three 2D NOE spectra, at mixing times $\tau_m =$ 40, 80, and 120 ms. For statistically meaningful results, the quadratic initial-slope approximation was repeated 10^4 times in the presence of 0.5% noise. The results, shown in Table 1, indicate that the quadratic initial-slope approximation always outperforms the relaxation-matrix analysis for the CR rate of $ARG^{37}\ H^{\gamma 2}-ARG^{24}\ H^{\beta 2}$ protons. For the CR rate of $ARG^{37}\ H^{\alpha}-TYR^{23}\ H^{\epsilon 1}$, the complete matrix treatment is superior, especially at long mixing times.

The importance of the effect of remote methylene protons is determined by the relative occurrence of remote methylene groups in native proteins. We studied the origin of short interproton distances ($r_{ij} < 5$ Å) in the following proteins: fasciculin 1 (*24*), C-terminal domain of cellobiohydrolase I (*26*), reduced thioredoxin (*27*), antiviral protein BDS-I (*28*), and complement control protein module (*29*). We found that 21–34% of all useful CR rates ($r_{ij} < 5$ Å), which are not fixed by the covalent geometry, are between remote methylene protons.

Our results can be summarized as follows. Although a complete matrix treatment takes into account spin diffusion (*11, 30*), it shows profound imperfections when spectral noise is taken into account. First, an increase in the size of the magnetization-exchange network steadily increases the uncertainty in determination of the relaxation matrix. Second, the effect of two strong CR rates on the connecting weak CR rate results in a large relative error in the determination of weak CR rates. This effect is expected to occur between remote methylene protons; in small globular proteins, it can affect up to one-third of all CR rates useful for structure determination. The quadratic initial-slope approximation (*6*) is relatively insensitive to both effects. Our results call for special attention to be paid to remote methylene protons in relaxation-matrix analysis and are particularly relevant for analysis at longer mixing times (*31, 32*).

ACKNOWLEDGMENT

We thank Dr. Steven B. Landy for valuable comments.

REFERENCES

1. A. Bax, *Annu. Rev. Biochem.* **58,** 223 (1989).
2. G. Wagner, *Prog. NMR Spectrosc.* **22,** 101 (1990).
3. S. Macura and R. R. Ernst, *Mol. Phys.* **41,** 95 (1980).
4. E. T. Olejniczak, R. T. Gampe, Jr., and S. W. Fesik, *J. Magn. Reson.* **67,** 28 (1980).
5. A. Kumar, G. Wagner, R. R. Ernst, and K. Wüthrich, *J. Am. Chem. Soc.* **103,** 3654 (1981).
6. J. Fejzo, Z. Zolnai, S. Macura, and J. L. Markley, *J. Magn. Reson.* **88,** 93 (1989).
7. C. M. Dobson, E. T. Olejniczak, F. M. Poulsen, and R. G. Ratcliffe, *J. Magn. Reson.* **48,** 97 (1982).
8. W. Massefski, Jr., and P. H. Bolton, *J. Magn. Reson.* **65,** 526 (1985).
9. R. Boelens, T. M. G. Koning, and R. Kaptein, *J. Mol. Struct.* **173,** 299 (1988).
10. B. A. Borgias and T. L. James, *J. Magn. Reson.* **79,** 493 (1988).
11. B. A. Borgias, M. Gochin, D. J. Kerwood, and T. L. James, *Prog. NMR Spectrosc.* **22,** 83 (1990).
12. M. Nilges, J. Habazettl, A. T. Brunger, and T. A. Holak, *J. Mol. Biol.* **219,** 499 (1991).
13. C. B. Post, R. P. Meadows, and D. G. Gorenstein, *J. Am. Chem. Soc.* **112,** 6796 (1990).
14. D. Kominos, A. K. Suri, D. B. Kitchen, D. Bassolino, and R. M. Levy, *J. Magn. Reson.* **97,** 398 (1992).
15. Y. Liu, D. Zhao, R. Altman, and O. Jardetzky, *J. Biomol. NMR* **2,** 373 (1992).
16. J. Tropp, *J. Chem. Phys.* **72,** 6035 (1980).
17. L. G. Werbelow and D. M. Grant, *Adv. Magn. Res.* **9,** 189 (1977).
18. R. Bruschweiler, ''Nuclear Magnetic Resonance Probes of Molecular Dynamics'' (R. Tycko, Ed.), Chap. 7, Kluwer Academic, Dordrecht/Norwell, Massachusetts, 1994.
19. S. Macura, *J. Magn. Reson. B* **104,** 168 (1994).
20. G. M. Clore and A. M. Gronenborn, *J. Magn. Reson.* **61,** 158 (1985).
21. S. B. Landy and B. D. Nageswara Rao, *J. Magn. Reson.* **83,** 29 (1989).
22. S. B. Landy and B. D. Nageswara Rao, *J. Magn. Reson. B* **102,** 209 (1993).
23. G. H. Weiss and J. A. Ferretti, *J. Magn. Reson.* **55,** 397 (1983).
24. M. H. le Du, P. Marchot, P. E. Bougis, and J. C. Fontecilla-Camps, *J. Biol. Chem.* **267,** 22122 (1992).
25. A. K. Suri and R. M. Levy, *J. Magn. Reson. B* **101,** 320 (1993).
26. P. J. Kraulis, G. M. Clore, M. Nilges, T. A. Jones, G. Pettersson, J. Knowles, and A. M. Gronenborn, *Biochemistry* **28,** 7241 (1989).
27. M.-F. Jeng, A. P. Campbell, T. Begley, A. Holmgren, D. A. Case, P. E. Wright, and H. J. Dyson, *Structure* **2,** 853 (1994).
28. P. C. Driscoll, A. M. Gronenborn, L. Beress, and G. M. Clore, *Biochemistry* **28,** 2188 (1989).
29. D. G. Norman, P. N. Barlow, M. Baron, A. J. Day, R. B. Sim, and I. D. Campbell, *J. Mol. Biol.* **219,** 717 (1991).
30. R. Kaptein, T. M. G. Koning, and R. Boelens, ''Computational Aspects of the Study of Biological Macromolecules by Nuclear Magnetic Resonance Spectroscopy'' (J. C. Hoch, Ed.), p. 349, Plenum Press, New York, 1991.
31. A. K. Suri and R. M. Levy, *J. Magn. Reson. B* **106,** 24 (1995).
32. P. D. Thomas, V. J. Basus, and T. L. James, *Proc. Natl. Acad. Sci. USA* **88,** 1237 (1991).